Psychological Medicine (2017), **47**, 1300–1310. © Cambridge University Press 2017
doi:10.1017/S0033291716003469

ORIGINAL ARTICLE

Abnormalities in the effective connectivity of visuothalamic circuitry in schizophrenia

S. J. Iwabuchi[1] and L. Palaniyappan[2,3,4]*

[1] *Translational Neuroimaging for Mental Health, Division of Psychiatry and Applied Psychology, University of Nottingham, Nottingham, UK*
[2] *Departments of Psychiatry & Medical Biophysics, University of Western Ontario, London, Ontario, Canada*
[3] *Robarts Research Institute & The Brain and Mind Institute, University of Western Ontario, London, Ontario, Canada*
[4] *Lawson Health Research Institute, London Ontario, Canada*

Background. Sensory-processing deficits appear crucial to the clinical expression of symptoms of schizophrenia. The visual cortex displays both dysconnectivity and aberrant spontaneous activity in patients with persistent symptoms and cognitive deficits. In this paper, we examine visual cortex in the context of the remerging notion of thalamic dysfunction in schizophrenia. We examined specific regional and longer-range abnormalities in sensory and thalamic circuits in schizophrenia, and whether these patterns are strong enough to discriminate symptomatic patients from controls.

Method. Using publicly available resting fMRI data of 71 controls and 62 schizophrenia patients, we derived conjunction maps of regional homogeneity (ReHo) and fractional amplitude of low-frequency fluctuations (fALFF) to inform further seed-based Granger causality analysis (GCA) to study effective connectivity patterns. ReHo, fALFF and GCA maps were entered into a multiple kernel learning classifier, to determine whether patterns of local and effective connectivity can differentiate controls from patients.

Results. Visual cortex shows both ReHo and fALFF reductions in patients. Visuothalamic effective connectivity in patients was significantly reduced. Local connectivity (ReHo) patterns discriminated patients from controls with the highest level of accuracy of 80.32%.

Conclusions. Both the inflow and outflow of Granger causal information between visual cortex and thalamus is affected in schizophrenia; this occurs in conjunction with highly discriminatory but localized dysconnectivity and reduced neural activity within the visual cortex. This may explain the visual-processing deficits that are present despite symptomatic remission in schizophrenia.

Received 2 August 2016; Revised 7 December 2016; Accepted 8 December 2016; First published online 12 January 2017

Key words: Effective connectivity, fractional amplitutude of low frequency fluctuations, machine learning, regional homogeneity, schizophrenia, visuothalamic.

Introduction

Impairments in processing sensory stimuli in patients with schizophrenia are now well documented, and these may underlie the more complex symptomatology such as hallucinations and delusions. Javitt & Freedman (2015) suggest that the failure to accurately process basic sensory information leads to an inevitable impact on neuronal mechanisms further down the processing stream in regions involved in higher order functions (Javitt, 2009). Studies using electroencephalogram (EEG) (Butler *et al.* 2007; Boutros *et al.* 2008), functional MRI (fMRI) (Jones, 1997; Woodward *et al.* 2012; Anticevic *et al.* 2014) and positron emission (Andreasen *et al.* 1996) have demonstrated dysfunctional communication between subcortical and cortical centres involved in processing sensory stimuli. While there is currently no consensus around the exact nature of connectivity disturbance in schizophrenia, it is now clear that brain-wide dysconnectivity is a hallmark of schizophrenia. Of particular interest is the connectivity of the thalamus to the rest of the brain since this forms multiple parallel pathways to relay information to and from the cortex (Behrens *et al.* 2003), and has recently been shown to be a key hub underlying the widespread network dysconnectivity in schizophrenia (Cheng *et al.* 2015).

Regional homogeneity (ReHo) and fractional amplitude of low-frequency fluctuations (fALFF) provide a measure of regional spontaneous brain activity, or 'local connectivity' and have also been shown to associate with connectivity of intrinsic networks with greatest amplitudes being observed in default mode regions (Zuo *et al.* 2010; Lin *et al.* 2015). In schizophrenia, studies

* Address for correspondence: Dr L. Palaniyappan, Prevention & Early Intervention Program for Psychoses (PEPP), A2-636, LHSC-VH, 800 Commissioners Road, London, Ontario N6A 5W9, Canada.
(Email: Lena.Palaniyappan@lhsc.on.ca)

using ReHo and fALFF are limited, although there is growing evidence for significant alterations across the brain, including consistent reductions in posterior sensory regions (Liu *et al.* 2006; Hoptman *et al.* 2010; Turner *et al.* 2013; Yu *et al.* 2013, 2014; Cheng *et al.* 2015; Xu *et al.* 2015). Interestingly, during n-back task performance, the distal functional connectivity of visual regions appear to be abnormally increased in schizophrenia compared to healthy controls and patients with bipolar disorder (Palaniyappan & Liddle, 2014), suggesting that abnormalities in visual cortex connectivity is likely to have spatially distributed impact on information processing tasks that are relevant to schizophrenia. Furthermore, structural abnormalities have also been reported including reduction in white-matter integrity, and various changes in gray-matter structure (Ananth *et al.* 2002; Narr *et al.* 2005; Onitsuka *et al.* 2007; Palaniyappan *et al.* 2013*a*; Guo *et al.* 2016). Recent work now suggests that there is a dysconnectivity between these occipital regions and the thalamus (Woodward *et al.* 2012; Anticevic *et al.* 2014; Klingner *et al.* 2014). Collectively, the literature thus far suggests that there are alterations in local connectivity within sensory regions, with concurrent aberrant longer-range connectivity with the thalamus. Here, we used a publicly available dataset acquired by the Centre for Biomedical Research Excellence (COBRE) to identify in patients with schizophrenia: (1) if dysfunctional spontaneous activity and localized connectivity co-occur in the visual cortex, (2) if directional differences exist in resting-state connectivity of the visuothalamic network. Additionally, we hypothesize that the patterns of local and directed connectivity of the visuothalamic circuitry can accurately discriminate patients from controls.

Materials and method

Participants

Data were acquired from a total of 147 subjects (75 healthy controls, 72 patients with schizophrenia). From these, two healthy controls withdrew from the study and a further two were not eligible. Ten patients were also excluded from the analyses due to excessive movement (>3 mm) during the scans. This resulted in a total of 133 subjects (71 healthy controls, 62 patients with schizophrenia). All subjects were screened and excluded if they had history of neurological disorder, history of mental retardation, history of severe head trauma with more than 5 min loss of consciousness, history of substance abuse or dependence within the last 12 months. Patients with co-morbid diagnoses of other Diagnostic Statistical Manual IV (DSM-IV) conditions were also excluded. The Structured Clinical Interview used for DSM Disorders (SCID) was used for diagnostic purposes. Demographic information is listed in Table 1. The authors assert that all procedures contributing to this work comply with the ethical standards of the relevant national and institutional committees on human experimentation and with the Helsinki Declaration of 1975, as revised in 2008.

Image acquisition and preprocessing

The COBRE dataset (http://fcon_1000.projects.nitrc.org/indi/retro/cobre.html) consisted of resting-state fMRI scans acquired on a 3 T Siemens Magnetom Trio MRI scanner using a single-shot full k-space echo-planar imaging (EPI) with ramp sampling correction using the intercomissural line (AC-PC) as a reference (TR: 2 s, TE: 29 ms, matrix size: 64 × 64, 32 slices, voxel size: $3 \times 3 \times 4$ mm^3). A multi-echo MPRAGE (MEMPR) sequence was also acquired with the following parameters: TR/TE/TI = 2530/(1.64, 3.5, 5.36, 7.22, 9.08)/900 ms, flip angle = 7°, FOV = 256 × 256 mm^2, Slab thickness = 176 mm, matrix size: 256 × 256, Voxel size: $1 \times 1 \times 1$ mm^3. With 5 echoes, the TR, TI and time to encode partitions for the MEMPR are similar to that of a conventional MPRAGE, resulting in similar GM/WM/CSF contrast.

The first five time-points of the resting-state data were discarded due to instability of the initial MRI signal, which left 145 volumes for processing. The data were preprocessed using the Data Processing Assistant for resting-state fMRI (DPARSF) package (Chao-Gan & Yu-Feng, 2010). First, images were slice-timing corrected. To correct for movement artefacts, we undertook a rigorous three-step approach. Next, we excluded any subjects with more than one voxel length of movement (3 mm or 3 degrees). Images were spatially realigned to the first image of each dataset and movement parameters were assessed for each subject and corrected using the rigid-body 6 approach (Friston *et al.* 1995). The data was scrubbed to further correct for movement artefacts using Frame-wise Displacement (FD, 0.5 mm) using a nearest-neighbour interpolation approach (Power *et al.* 2012). We also compared FD values between groups and found that patients (mean = 0.37, S.D. = 0.19) were significantly higher than controls (mean = 0.27, S.D. = 0.15). We therefore entered these values as covariates in the subsequent ANOVA. No significant correlation was observed between FD and the extracted values for ReHo (controls: $r = -0.18$, $p = 0.13$; patients: $r = -0.16$, $p = 0.21$), fALFF (controls: $r = 0.03$, $p = 0.8$; patients: $r = -0.12$, $p = 0.35$) or GCA seeded from cuneus (controls: $r = 0.04$, $p = 0.71$; patients: $r = 0.13$, $p = 0.32$) and thalamus (controls: $r = 0.16$, $p = 0.17$; patients: $r = -0.02$,

https://doi.org/10.1017/S0033291716003469 Published online by Cambridge University Press

Table 1. *Demographics of healthy control and patient subjects*

	Healthy control ($n = 71$)		Schizophrenia ($n = 62$)		
Measure	Mean	S.D.	Mean	S.D.	p
Age (years)	35.96	11.8	38.37	14.2	0.29
Gender					0.18
Male	50		50		
Female	21		12		
Handedness					<0.05
Right	68		50		
Left	1		10		
Both	2		2		
IQ					
Verbal	105.8	14.72	99.29	16.72	0.02
Performance	116.18	15.62	103.45	16.91	<0.001
Sum	112.44	11.49	100.78	17.37	<0.001
Education (years)	14.24	2.68	13.19	1.81	0.01
Illness duration (years)	–	–	16.5	13.22	
CPZ equivalents[a]	–	–	366.51	309.5	
PANSS					
Positive	–	–	12.16	4.62	
Negative	–	–	15.2	6.13	
Total	–	–	49.87	11.33	

CPZ, Chlorpromazine; IQ, intelligence quotient; PANSS, Positive and Negative Syndrome Scale; S.D., standard deviation.
[a] Chlorpromazine equivalents of current medications calculated according to dose equivalences provided by COBRE investigators based on Andreasen *et al.* (2010) and reported by Yang *et al.* (2014)

$p = 0.87$). White matter and CSF signal were both regressed out as nuisance covariates. DARTEL (Ashburner, 2007) was used to normalize the data using each subject's structural image before removing linear drift. For fALFF calculation, the data were spatially smoothed using a 4 mm FWHM Gaussian kernel. The smoothing for ReHo was applied last in the pipeline prior to higher level analysis. We then applied a band-pass filter (0.01–0.08 Hz) to remove low-frequency fluctuations and high-frequency noise.

Reho and fALFF analyses

Both ReHo and fALFF maps were generated using the DPARSF package. ReHo was calculated for each subject by calculating Kendall's coefficient of concordance of each voxel's time-course with those of its nearest neighbours (26 voxels) (Zang *et al.* 2004). For fALFF, the time series of each voxel was transformed to the frequency domain to determine the power spectrum, and the sum of amplitude of the low-frequency range determines ALFF. fALFF maps were calculated for each subject as the proportion of power spectrum of low frequency (0.01–0.08 Hz) across the entire frequency range (Zou *et al.* 2008). The ReHo and fALFF maps were then z-transformed for the higher-level analyses.

Conjunction analysis

We first identified regions with significant difference between groups for both ReHo and fALFF [family-wise error (FWE)-corrected, $p < 0.05$] and found clusters located in the cuneus and postcentral gyrus for both ReHo and fALFF, and additionally the thalamus for the ReHo analysis, showing attenuation in patients compared to controls (Supplementary Fig. S1). To visualize the spatial overlap of group differences across ReHo and fALFF, the statistical parametric maps of both modalities were thresholded at $p < 0.001$ uncorrected and the intersection between the two were determined as voxels contained in both maps with a cluster extent threshold 150 voxels. Since the use of FWE-corrected maps for the conjunction makes it very unlikely that overlapping regions are found, and further lowers consistency of overlap (Duncan *et al.* 2009), a more liberal and uncorrected threshold was used. However, in order to minimize type I error, we also determined a cluster threshold by calculating cluster size threshold estimation for ReHo and fALFF maps which produced 18 and 84 voxels, respectively. Both methods resulted in the same cluster in the cuneus. The cuneus cluster was then used to create a spherical region of interest (ROI) as a seed region for Granger causality analysis (GCA).

https://doi.org/10.1017/S0033291716003469 Published online by Cambridge University Press

Granger causality analysis

GCA provides a measure of effective connectivity whereby Granger causal connectivity between two regions indicates that neuronal activity of one region is predictive of activity that occurs in another region. We used a 6-mm radius sphere centred on the peak of the cuneus cluster (MNI: 0, −84, 24) identified from the conjunction analysis to determine effective connectivity of this region to the rest of the brain. The comparison between groups resulted in a significant cluster in the thalamus. We also then ran a reverse GCA seeding from this significant thalamic cluster to identify effective connectivity from the thalamic cluster back to the cuneus. Detailed procedures for the GCA analysis are reported in a previous study (Iwabuchi *et al.* 2014).

Statistical analysis

The z-transformed GCA maps seeded from the ROIs were subjected to whole-brain voxelwise analysis using SPM8 to identify differences in effective connectivity from the cuneus to the rest of the brain between schizophrenia patients and controls. Since we were specifically interested in visuothalamic connections, for the voxel-wise analysis, we used the corresponding small-volume correction mask of the visual thalamic mask taken from the Oxford thalamic probability atlas (Behrens *et al.* 2003) which are structural connectivity-based subdivisions of the thalamus based on probabilistic tractography. We also extracted mean GCA coefficients from the cuneus and thalamus seed masks from the *z*-transformed x-to-y GCA maps to identify group differences in directional influence between the two regions maps (i.e. mean of thalamus ROI from GCA seeded from cuneus; mean of cuneus ROI from GCA seeded from thalamus). The GCA coefficients were entered into a repeated-measures ANOVA with direction (cuneus-to-thalamus and thalamus-to-cuneus) as within-subject factor and group (control and patient) as between subject factor. We also extracted mean ReHo and fALFF values from the cuneus seed used in the GCA to explore associations between these measures and the directional influence between the cuneus and thalamus using Spearman's correlation (as thalamus-to-cuneus GCA was not normally distributed). To rule out effects of medication, the GCA coefficients were correlated with current antipsychotic dose as measured by chlorpromazine (CPZ) equivalents. We also explored whether there are any relationships between visuothalamic connectivity (Granger coefficients in either direction, and ReHo and fALFF values extracted from the cuneus) and PANSS scores and illness duration. All statistical analyses were performed on IBM SPSS v. 21.0 (IBM Corp., USA) for Windows and used an α-level of 0.05 (correlation analyses were corrected for multiple comparisons using the Holm–Bonferroni correction).

Classification

The classification analysis was carried out using Pattern Recognition for Neuroimaging Toolbox (PRoNTo) (http://www.mlnl.cs.ucl.ac.uk/pronto). The ReHo, fALFF and GCA maps seeded from both the cuneus and thalamus were entered as separate modalities into a multiple kernel learning (MKL) classifier, which is based on a support vector machine algorithm. Separate linear kernels were built for each modality and features were mean-centred using training data and kernels were normalized. The outer loop for assessing the model's performance used a leave one subject out per group cross-validation approach. To validate and assess performance of the classifier, cross validation was performed in a double nested loop. The inner loop was used for the parameter optimization using a *k*-fold cross-validation approach on subjects per-group out with $k = 5$. This optimizes the soft-margin parameter *C* and provides good generalizability via a bias-variance trade-off (James *et al.* 2013). Values of parameter *C* were 0.01, 0.1, 1, 10 and 100. The value of *C* that was selected most frequently for each model was as follows: ReHo: 100; fALFF: 1; GCA: 1; ReHo + fALFF: 100; ReHo + GCA: 1; ReHo + fALFF + GCA: 100 (although it should be noted that the value of *C* may not have been the same for all folds). The outer loop for assessing the model's performance used a leave one subject per group out cross validation approach. We obtained values for balanced accuracy, specificity, sensitivity, predictive values and area under the receiver operator curve (AUC) and statistical significance of these measures was determined by way of permutation testing ($n = 1000$ permutations with random assignment of patient/control labels to the training data) using $p < 0.05$).

Results

Effective connectivity

Analyses revealed significantly higher cuneus–thalamus (left) effective connectivity in controls compared to patients ($p < 0.05$, FWE corrected, $k > 5$) using a small-volume correction (SVC) of the visual-thalamic mask (Fig. 1*a*, Supplementary Fig. S2 and Table S2). The whole-brain analysis for GCA seeded from the thalamus showed a significant cluster of higher GCA coefficient in patients compared to controls in the right visual association area ($p < 0.05$, FWE corrected) (Fig. 1*b* and Table 2). SVC using the cuneus seed

https://doi.org/10.1017/S0033291716003469 Published online by Cambridge University Press

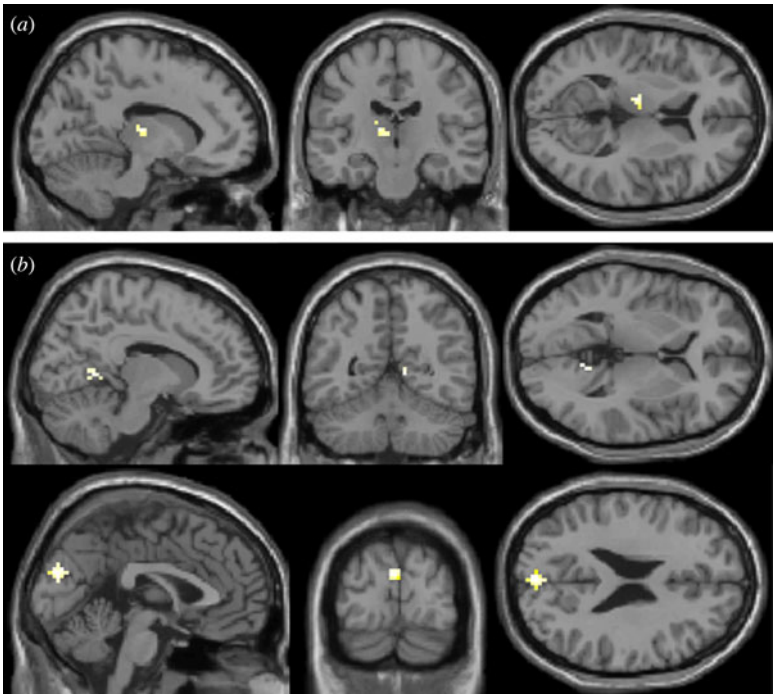

Fig. 1. (*a*) Thalamus cluster showing greater effective connectivity from the cuneus seed region of interest (ROI) in controls compared to patients [significant at $p < 0.05$, family-wise error (FWE) corrected, $k > 5$]. (*b*) Visual association cortex cluster (top) and cuneus cluster (bottom) showing greater effective connectivity from the thalamus seed ROI in patients compared to controls (significant at $p < 0.05$, FWE corrected, $k > 5$).

Table 2. *Regions showing significantly altered effective connectivity in patients compared to controls from the cuneus and thalamus seed regions (significant at p < 0.05, FWE corrected)*

Region	MNI (x, y, z)	Brodmann's area	*T*	Voxels
Cuneus seed to				
Left thalamus	−12, −18, 9	50	3.95[a]	17
Thalamus seed to				
Right visual association area	12, −54, 3	18	5.36	9
Cuneus	0, −87, 24	18	4.77[a]	33

[a] Small volume corrected at $p < 0.05$, family-wise error (FWE) corrected.

mask also revealed a significant cluster in the cuneus region ($p < 0.05$, FWE corrected).

The repeated-measures ANOVA revealed significant interaction for group and direction ($F_{1130} = 22.28$, $p < 0.001$). Specifically, for the cuneus thalamus connectivity, controls showed a positive influence (mean = 0.8, S.D. = 1.68) while patients showed a negative influence (mean = −0.3, S.D. = 1.25) ($p < 0.001$). Conversely, the thalamus-cuneus connectivity showed a negative influence in controls (mean = −1.7, S.D. = 2.85) and a positive influence in patients (mean = 0.25, S.D. = 1.66) ($p < 0.001$). Furthermore, while controls showed a significantly opposing directional influence between the cuneus and thalamus ($p < 0.001$), patients did not show such a pattern ($p = 0.25$). The correlation of influence between the two directions is highly correlated in both controls and patients ($r = -0.61$ and $r = -0.69$, respectively, both $p < 0.001$); however, on closer inspection, the inflow/outflow index (indexed by thalamus-cuneus influence subtracted by cuneus-thalamus influence) is significantly diminished in patients ($p < 0.001$). Furthermore, a one-sample *t* test also revealed that Granger coefficients in both directions of the patient group did not differ significantly from zero ($p > 0.05$), suggesting very weak connectivity between the thalamus and cuneus. Healthy controls on the other hand showed significant strength of connectivity in both directions ($p < 0.001$). Results are summarized in Table 3. Both mean ReHo and fALFF

https://doi.org/10.1017/S0033291716003469 Published online by Cambridge University Press

Table 3. *Mean GCA coefficients in the cuneus and thalamus in controls and patients*

	Mean GCA coefficient (S.D.)		
Direction	Controls	Patients	*p*
Cuneus to thalamus flow	0.8 (1.68)	−0.3 (1.25)	<0.001
Thalamus to cuneus flow	−1.7 (2.85)	0.25 (1.67)	<0.001
Cuneus inflow/outflow index	−2.5 (4.09)	0.56 (2.69)	<0.001

GCA, Granger causality analysis.

of the cuneus seed correlated significantly with the inflow/outflow index in controls ($r = -0.32$, $p < 0.01$ and $r = -0.25$, $p < 0.05$, respectively) while this was diminished in patients ($r = -0.16$, $p > 0.05$ and $r = -0.09$, $p > 0.05$, respectively). Correlation with each direction separately revealed that this association was driven solely by the thalamus-cuneus influence (controls: $r = -0.35$, $p < 0.005$ and $r = -0.3$, $p < 0.05$, patients: $r = -0.15$, $p > 0.05$ and $r = -0.1$, $p > 0.05$ for ReHo and fALFF, respectively) (cuneus-thalamus was not significantly correlated in either group). This is depicted in Fig. 2. There were no significant correlations between CPZ equivalents and Granger coefficients in either direction ($p = 0.75$ and 0.58 for cuneus-thalamus and thalamus-cuneus, respectively), suggesting that differences in connectivity are not due to antipsychotic medication. Neither the clinical scores nor illness duration correlated significantly with local connectivity or effective connectivity in either direction (all $p > 0.1$).

Classification

The MKL classifier using ReHo, fALFF and GCA maps in both directions performed with a balanced accuracy of 76.74% with specificity of 76.06% and sensitivity of 77.42% with an area under the curve of 86%. The contribution for each modality was as follows: ReHo = 32.57%, fALFF = 35.65%, cuneus to thalamus GCA = 17.98%, thalamus to cuneus GCA = 13.81%. Based on this, we also ran the classifier for ReHo and fALFF both separately and combined to see whether GCA maps improved classification accuracy. ReHo alone yielded an accuracy of 78.04% (80.28% specificity, 75.81% sensitivity) while fALFF resulted in an accuracy of 70.39% (74.65% specificity, 66.13% sensitivity). ReHo and fALFF combined in the model provided an accuracy of 77.94% (81.69% specificity, 74.19% sensitivity). Combining the two best modalities of GCA and ReHo resulted in an accuracy of 76.14% (73.24% specificity, 79.03% sensitivity) with an area under the curve of 85%. Results are summarized in Table 4.

Discussion

We note several findings relevant to the occipital cortex physiology in schizophrenia, that are, to our knowledge, hitherto unreported. In patients, there is significantly reduced low-frequency signal amplitude, co-occurring with reduced local connectivity within the occipital regions, which is also accompanied by an abnormal pattern of effective connectivity between this region and the thalamus at resting state. While controls exhibited a strong positive influence from cuneus to thalamus along with a strong negative influence from the thalamus back to the cuneus, patients showed substantially weakened connectivity of this thalamo-cortical feedback circuit. In addition, ReHo also provided high discriminatory accuracy between the two groups, with the highest sensitivity (correctly labelling a patient as a patient) achieved with the combination of ReHo and GCA maps, suggesting these modalities may be valuable in the search for biological markers for schizophrenia.

Local connectivity

Our ReHo and fALFF conjunction analysis showing reductions in the cuneus are consistent with previous literature employing similar methods, albeit in isolation, to study patients with schizophrenia (Hoptman *et al.* 2010; Liu *et al.* 2010; Turner *et al.* 2013; Yu *et al.* 2013, 2014; Xu *et al.* 2015). In schizophrenia, decreases in fALFF seem to be more consistently reported than increases, and tend to occur in posterior regions including occipital and precuneus/cuneus regions (Hoptman *et al.* 2010; Turner *et al.* 2013; Yu *et al.* 2014). Similarly, ReHo has also shown reductions in occipital regions (Liu *et al.* 2010; Yu *et al.* 2013). A recent meta-analysis of studies investigating ReHo and ALFF/fALFF alterations in schizophrenia also showed decreased levels in the occipital cortex (Xu *et al.* 2015). A similar measure of resting-state functional connectivity density, which measures the connectivity of a single voxel with all other brain voxels, has also shown to be reduced specifically in the occipital cortex in schizophrenia (Zhuo *et al.* 2014). Also of relevance is a report of increased centrality in schizophrenia (but not in bipolar disorder) notable in the occipital cortex, suggesting that the redistribution of the global connectivity of the visual cortex is a consistent feature of schizophrenia (Palaniyappan & Liddle, 2014). In line with this finding of aberrant visual cortex connections, input from the visual regions to the insula has also shown to be diminished in schizophrenia (Palaniyappan *et al.* 2013*b*), indicating cross-network sensory-processing disruptions. Further, steady-state visual evoked potential studies have demonstrated strong evidence for magnocellular dysfunction showing early-stage visual-processing deficits, which likely

https://doi.org/10.1017/S0033291716003469 Published online by Cambridge University Press

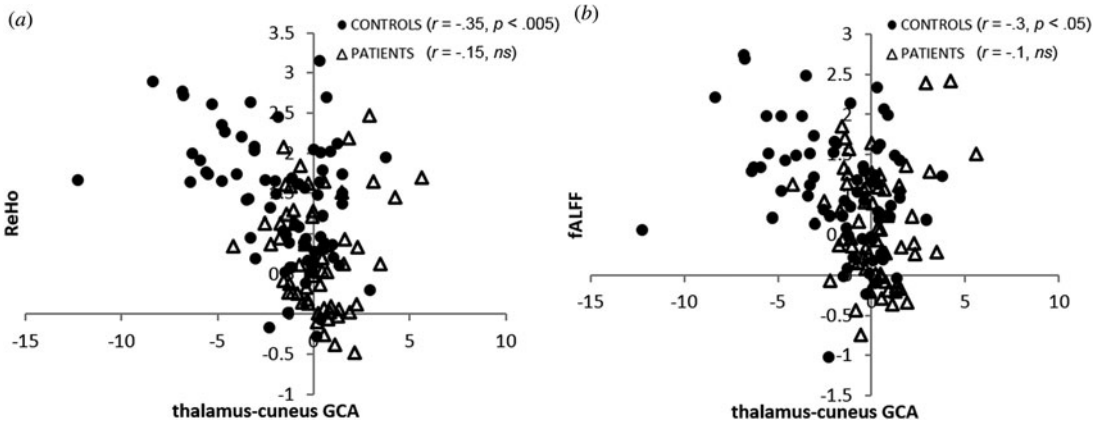

Fig. 2. Spearman's correlation between mean (*a*) regional homogeneity (ReHo) and (*b*) fractional amplitude of low-frequency fluctuations (fALFF) of the cuneus seed and Granger causality analysis (GCA) coefficients of cuneus seeded from the thalamus.

Table 4. *Balanced accuracy, sensitivity, specificity and area under curve for multiple kernel learning classifier using ReHo, fALFF and GCA maps*

Modality	Accuracy (%)	Specificity (%)	Sensitivity (%)	AUC (%)	*p* value
ReHo	78.04	80.28	75.81	86	0.001
fALFF	70.39	74.65	66.13	82	0.001
GCA	71.4	71.83	70.97	80	0.001
ReHo + fALFF	77.94	81.69	74.19	87	0.001
ReHo + GCA	76.14	73.24	79.03	85	0.001
ReHo + fALFF + GCA	76.74	76.06	77.42	86	0.001

ReHo, Regional homogeneity; fALFF, fractional amplitude of low-frequency fluctuations; GCA, Granger causality analysis.

contribute to impairments further up the cognitive and social processing stream resulting in global dysfunction in schizophrenia (Butler & Javitt, 2005). To support, Wynn *et al*. (2008) reported abnormal functional topography of the lateral occipital cortex in patients which they suggest may relate to impaired ability in object recognition tasks.

Effective connectivity

Studies thus far have indicated a dissociation of undirected thalamo-cortical functional connectivity between prefrontal and sensory networks characterized by thalamic hyperconnectivity with motor and sensory regions (Woodward *et al.* 2012; Anticevic *et al.* 2014). We note that this relative hyperconnectivity is actually directed from thalamus to visual areas, with net cuneus inflow/outflow being above zero in patients, while being below zero in healthy controls. In general, similar work has predominantly focused on prefrontal-thalamic coupling, with few studies specifically exploring visual-thalamic pathways despite aforementioned reports of visual processing impairment in schizophrenia. However, one recent study using whole brain approach to study the connectivity of the thalamus to cortical ROIs found greater coupling of fronto-thalamic circuits, as well as an absence of negative correlations between the thalamus and sensory and motor regions in schizophrenia (Klingner *et al.* 2014). This lack of negative correlation holds true for our data where the strong negative influence from the thalamus to cuneus observed in controls is completely diminished in the patients. Anticevic *et al.* (2012) have previously proposed a mechanism via cortical disinhibition to account for the disrupted long-range cortico-cortical connectivity, and further explain the possibility of aberrant brain-wide balance of excitation and inhibition which disrupts the relay of information between the thalamus and cortex (Anticevic *et al.* 2014). This widespread alteration of inhibitory and excitatory balance has indeed been observed in both magnetic resonance spectroscopy studies in schizophrenia as well as animal models (Krystal *et al.* 2003; Kehrer *et al.* 2008; Jardri & Denève 2013; Schobel *et al.* 2013; Marsman *et al.* 2014; Taylor & Tso, 2015), consistent with the NMDA receptor hypofunction

https://doi.org/10.1017/S0033291716003469 Published online by Cambridge University Press

model. Functionally, negative correlations between brain regions have been thought to subserve inhibitory interactions where strength of anti-correlations are related to cognitive performance (Kelly *et al.* 2008; Hampson *et al.* 2010). Given that glutamate is the primary neurotransmitter within the visual system, combined with glutamatergic theories of schizophrenia (Javitt, 2010), it would be of great interest to investigate whether disrupted ReHo and fALFF relate to levels of glutamate in the visual cortex. To date, studies of occipital neurochemistry in schizophrenia are limited and both methodology and findings are vastly inconsistent (Chang *et al.* 2007; Marsman *et al.* 2014). Combining modalities in the same dataset is essential for the development of a more complete understanding for the mechanisms underlying sensory dysfunction in schizophrenia.

Association between local and distal connectivity

Interestingly, our analyses revealed a loss in association between the thalamus–cuneus influence and local connectivity measures in patients, suggesting a diminished interaction between spontaneous activity within the occipital region and the input from the thalamus. In controls, greater local connectivity and spontaneous activity is related to stronger negative influence of the thalamus on the cuneus, however this pattern is not reflected in patients. If local connectivity measured using BOLD is reflective of local excitation/inhibition balance as claimed recently using computational approaches (Deco *et al.* 2014), then it is intriguing to note that such local balance in the visual cortex could be influenced by thalamic input in patients more than controls. Obviously, it is not entirely possible to deduce from the current data whether the breakdown occurs in the cuneus, the thalamus or elsewhere, though it is evident that the circuit failure exists at both a regional and distal level of connectivity. Taken together, these findings collectively suggest that there is a breakdown of the interaction between the thalamus and cortex, which might be attributed to a mechanism of disinhibition, resulting in a brain-wide excitation/inhibition imbalance, and ultimately resulting in the global and multi-faceted impairments and symptomatology of schizophrenia.

Classification using connectivity maps

Studies using machine learning to discriminate schizophrenia from controls using resting state fMRI are growing though to date have been relatively limited (Shen *et al.* 2010; Venkataraman *et al.* 2012; Arbabshirani *et al.* 2013; Wang *et al.* 2015). In a recent meta-analysis of machine learning approaches discriminating patients with schizophrenia from controls, classification accuracies vary between 64–94% for sensitivity and 65–98% for specificity (Kambeitz *et al.* 2015), though this is likely attributed to the diversity in type of classifier used and parameters selected, as well as the heterogeneity of samples studied. Shen *et al.* (2010) used an ROI-based functional connectivity approach to discriminate patients from controls and achieved high total accuracy of 93.75% for discriminating patients (sensitivity), though specificity reached only 75%. Similarly, Arbabshirani *et al.* (2013) also attained high accuracy of up to 96% (92% specificity, 100% sensitivity) using functional connectivity of major resting state networks. However, more modest accuracies around 75% have also been reported using similar inputs of resting state functional connectivity for machine learning (Venkataraman *et al.* 2012; Wang *et al.* 2015). Our study, using a multiple kernel learning SVM approach to determine contributions of the three resting-state fMRI measures achieved accuracies that lie between these previous reports, with ReHo achieving the best performance for overall accuracy. We aware of only one previous study using ReHo and fALFF to discriminate schizophrenia patients from control. Chyzhyk *et al.* (2015) were able to discriminate patients from controls with a very high accuracy reaching 97 and 100% for ReHo and fALFF respectively. Surprisingly, the most highly performing classifier (100%) used ReHo to discriminate schizophrenia patients with auditory hallucinations from those without. However, the sample size in this study was much smaller than the current study, which is known to produce higher accuracy rates due to sample homogeneity (Schnack & Kahn, 2016). Larger samples often have lower accuracy, but are more generalizable to other samples, which is vital with regards to clinically translatable findings. Therefore, although functional connectivity is often utilized for pattern classification of mental disorders, local connectivity may be a potential biomarker to consider for clinically diagnosing schizophrenia. Furthermore, it is possible that the combination of both local and longer-range connectivity indices might differentiate the subtle brain-wide pathophysiology better than one modality alone. The challenge will be to determine the exact measures that will enable the best discriminatory ability.

One of the issues in the current study, as well as many others in the field, is the effect of medication. While we cannot completely eliminate the potential confounding effects of medication, we found that medication was not associated with effective connectivity, suggesting that these changes are unlikely to be driven by medication. Furthermore, illness duration also did not show an association with thalamo-cortical connectivity, which indicates that this change might precede illness onset. Findings of (Anticevic *et al.* 2015) support

https://doi.org/10.1017/S0033291716003469 Published online by Cambridge University Press

such a notion where they reported dysconnectivity of the thalamo-cortical circuitry in those at risk for psychosis. Moreover, those who converted to full-blown psychosis had the most profound dysfunction, which has significant implications for considering thalamo-cortical connectivity in prognosis for schizophrenia. This idea might also explain the lack of association observed between symptom measures and IQ and effective connectivity, where aberrant communication between the cuneus and thalamus already exists prior to more externally visible characteristics of the disorder.

To summarize, we have observed a crucial physiological aberration in the visual cortex in schizophrenia, and highlighted the potential clinical utility of the observation in discriminating a patient with schizophrenia compared to a healthy control. We wish to highlight that occipital regions, as well as the prefrontal cortex, are amenable to noninvasive neuromodulation by virtue of their vicinity to the scalp surface. Experimental studies to investigate the ability of brain stimulation approaches to modify the physiological changes highlighted here would offer a potential means to move towards therapeutic translation.

Supplementary material

The supplementary material for this article can be found at https://doi.org/10.1017/S0033291716003469

Acknowledgements

Wellcome Trust (grant no. 076448/Z/05/Z). Department of Psychiatry & Schulich School of Medicine Dean's Support funds, Western University, Ontario. People Programme (Marie Curie Actions) of the European Union's Seventh Framework Programme (FP7/2007-2013) under REA grant agreement no. PCOFUND-GA-2012-600181.

L.P. was previously supported by a Grant from the Wellcome Trust (grant no. 076448/Z/05/Z) and currently by the Department of Psychiatry & Schulich School of Medicine Dean's Support funds, Western University, Ontario. S.I. has received funding from the People Programme (Marie Curie Actions) of the European Union's Seventh Framework Programme (FP7/2007-2013) under REA grant agreement no. PCOFUND-GA-2012-600181.

Declaration of Interest

S.I. declares no conflict of interest. L.P. received a Young Investigator travel fellowship sponsored by Eli Lilly (2010) and Travel Support from Magstim Limited (2014) and in the last year, has held shares of Shire Inc. and GlaxoSmithKline in his spousal pension funds. L.P. is also supported by the Bucke Family Fund and the Academic Medical Organization of Southwestern Ontario (AMOSO).

References

Ananth H, Popescu I, Critchley HD, Good CD, Frackowiak RSJ, Dolan RJ (2002). Cortical and subcortical gray matter abnormalities in schizophrenia determined through structural magnetic resonance imaging with optimized volumetric voxel-based morphometry. *American Journal of Psychiatry* **159**, 1497–1505.

Andreasen NC, O'Leary DS, Cizadlo T, Arndt S, Rezai K, Ponto LL, Watkins GL, Hichwa RD (1996). Schizophrenia and cognitive dysmetria: a positron-emission tomography study of dysfunctional prefrontal-thalamic-cerebellar circuitry. *Proceedings of the National Academy of Sciences USA* **93**, 9985–9990.

Andreasen NC, Pressler M, Nopoulos P, Miller D, Ho B-C (2010). Antipsychotic dose equivalents and dose-years: a standardized method for comparing exposure to different drugs. *Biological Psychiatry* **67**, 255–262.

Anticevic A, Cole MW, Repovs G, Murray JD, Brumbaugh MS, Winkler AM, Savic A, Krystal JH, Pearlson GD, Glahn DC (2014). Characterizing thalamo-cortical disturbances in schizophrenia and bipolar illness. *Cerebral Cortex* **24**, 3116–3130.

Anticevic A, Gancsos M, Murray JD, Repovs G, Driesen NR, Ennis DJ, Niciu MJ, Morgan PT, Surti TS, Bloch MH, Ramani R, Smith MA, Wang X-J, Krystal JH, Corlett PR (2012). NMDA receptor function in large-scale anticorrelated neural systems with implications for cognition and schizophrenia. *Proceedings of the National Academy of Sciences USA* **109**, 16720–16725.

Anticevic A, Haut K, Murray JD, Repovs G, Yang GJ, Diehl C, McEwen SC, Bearden CE, Addington J, Goodyear B, Cadenhead KS, Mirzakhanian H, Cornblatt BA, Olvet D, Mathalon DH, McGlashan TH, Perkins DO, Belger A, Seidman LJ, Tsuang MT, van Erp TG, Walker EF, Hamann S, Woods SW, Qiu M, Cannon TD (2015). Association of thalamic dysconnectivity and conversion to psychosis in youth and young adults at elevated clinical risk. *JAMA Psychiatry* **72**.

Arbabshirani MR, Kiehl KA, Pearlson GD, Calhoun VD (2013). Classification of schizophrenia patients based on resting-state functional network connectivity. *Frontiers in Neuroscience* **7**, 133.

Ashburner J (2007). A fast diffeomorphic image registration algorithm. *NeuroImage* **38**, 95–113.

Behrens TEJ, Johansen-Berg H, Woolrich MW, Smith SM, Wheeler-Kingshott CAM, Boulby PA, Barker GJ, Sillery EL, Sheehan K, Ciccarelli O, Thompson AJ, Brady JM, Matthews PM (2003). Non-invasive mapping of connections between human thalamus and cortex using diffusion imaging. *Nature Neuroscience* **6**, 750–757.

Boutros NN, Arfken C, Galderisi S, Warrick J, Pratt G, Iacono W (2008). The status of spectral EEG abnormality as a diagnostic test for schizophrenia. *Schizophrenia Research* **99**, 225–237.

Butler PD, Javitt DC (2005). Early-stage visual processing deficits in schizophrenia. *Current Opinion in Psychiatry* **18**, 151–157.

Butler PD, Martinez A, Foxe JJ, Kim D, Zemon V, Silipo G, Mahoney J, Shpaner M, Jalbrzikowski M, Javitt DC (2007). Subcortical visual dysfunction in schizophrenia drives secondary cortical impairments. *Brain* **130**, 417–430.

Chang L, Friedman J, Ernst T, Zhong K, Tsopelas ND, Davis K (2007). Brain metabolite abnormalities in the white matter of elderly schizophrenic subjects: implication for glial dysfunction. *Biological Psychiatry* **62**, 1396–1404.

Chao-Gan Y, Yu-Feng Z (2010). DPARSF: a MATLAB toolbox for 'Pipeline' data analysis of resting-state fMRI. *Frontiers in Systems Neuroscience* **4**, 13.

Cheng W, Palaniyappan L, Li M, Kendrick KM, Zhang J, Luo Q, Liu Z, Yu R, Deng W, Wang Q, Ma X, Guo W, Francis S, Liddle P, Mayer AR, Schumann G, Li T, Feng J (2015). Voxel-based, brain-wide association study of aberrant functional connectivity in schizophrenia implicates thalamocortical circuitry. *npj Schizophrenia* **1**, 15016.

Chyzhyk D, Graña M, Öngür D, Shinn AK (2015). Discrimination of schizophrenia auditory hallucinators by machine learning of resting-state functional MRI. *International Journal of Neural Systems* **25**, 1550007.

Deco G, Ponce-Alvarez A, Hagmann P, Romani GL, Mantini D, Corbetta M (2014). How local excitation–inhibition ratio impacts the whole brain dynamics. *Journal of Neuroscience* **34**, 7886–7898.

Duncan KJ, Pattamadilok C, Knierim I, Devlin JT (2009). Consistency and variability in functional localisers. *NeuroImage* **46**, 1018–1026.

Friston KJ, Ashburner J, Frith CD, Poline J-B, Heather JD, Frackowiak RSJ (1995). Spatial registration and normalization of images. *Human Brain Mapping* **3**, 165–189.

Guo S, Palaniyappan L, Liddle PF, Feng J (2016). Dynamic cerebral reorganization in the pathophysiology of schizophrenia: a MRI-derived cortical thickness study. *Psychological Medicine* **46**, 1–14.

Hampson M, Driesen N, Roth JK, Gore JC, Constable RT (2010). Functional connectivity between task-positive and task-negative brain areas and its relation to working memory performance. *Magnetic Resonance Imaging* **28**, 1051–1057.

Hoptman MJ, Zuo X-N, Butler PD, Javitt DC, D'Angelo D, Mauro CJ, Milham MP (2010). Amplitude of low-frequency oscillations in schizophrenia: a resting state fMRI study. *Schizophrenia Research* **117**, 13–20.

Iwabuchi SJ, Peng D, Fang Y, Jiang K, Liddle EB, Liddle PF, Palaniyappan L (2014). Alterations in effective connectivity anchored on the insula in major depressive disorder. *European Neuropsychopharmacology*. **24**

James G, Witten D, Hastie T, Tibshirani R (2013). *An Introduction to Statistical Learning*, vol. **103**. Springer Texts in Statistics: Springer New York: New York, NY.

Jardri R, Denève S (2013). Circular inferences in schizophrenia. *Brain* **136**, 3227–3241.

Javitt DC (2009). Sensory processing in schizophrenia: neither simple nor intact. *Schizophrenia Bulletin* **35**, 1059–1064.

Javitt DC (2010). Glutamatergic theories of schizophrenia. *Israel Journal of Psychiatry and Related Sciences* **47**, 4–16.

Javitt DC, Freedman R (2015). Sensory processing dysfunction in the personal experience and neuronal machinery of schizophrenia. *American Journal of Psychiatry* **172**, 17–31.

Jones EG (1997). Cortical development and thalamic pathology in schizophrenia. *Schizophrenia Bulletin* **23**, 483–501.

Kambeitz J, Kambeitz-Ilankovic L, Leucht S, Wood S, Davatzikos C, Malchow B, Falkai P, Koutsouleris N (2015). Detecting neuroimaging biomarkers for schizophrenia: a meta-analysis of multivariate pattern recognition studies. *Neuropsychopharmacology* **40**, 1742–1751.

Kehrer C, Maziashvili N, Dugladze T, Gloveli T (2008). Altered excitatory-inhibitory balance in the NMDA-Hypofunction model of schizophrenia. *Frontiers in Molecular Neuroscience* **1**.

Kelly AMC, Uddin LQ, Biswal BB, Castellanos FX, Milham MP (2008). Competition between functional brain networks mediates behavioral variability. *NeuroImage* **39**, 527–537.

Klingner CM, Langbein K, Dietzek M, Smesny S, Witte OW, Sauer H, Nenadic I (2014). Thalamocortical connectivity during resting state in schizophrenia. *European Archives of Psychiatry and Clinical Neuroscience* **264**, 111–119.

Krystal JH, D'Souza DC, Mathalon D, Perry E, Belger A, Hoffman R (2003). NMDA receptor antagonist effects, cortical glutamatergic function, and schizophrenia: toward a paradigm shift in medication development. *Psychopharmacology* **169**, 215–233.

Lin F-H, Chu Y-H, Hsu Y-C, Lin J-FL, Tsai KW-K, Tsai S-Y, Kuo W-J (2015). Significant feed-forward connectivity revealed by high frequency components of BOLD fMRI signals. *NeuroImage* **121**, 69–77.

Liu H, Liu Z, Liang M, Hao Y, Tan L, Kuang F, Yi Y, Xu L, Jiang T (2006). Decreased regional homogeneity in schizophrenia: a resting state functional magnetic resonance imaging study. *Neuroreport* **17**, 19–22.

Liu Z, Xu C, Xu Y, Wang Y, Zhao B, Lv Y, Cao X, Zhang K, Du C (2010). Decreased regional homogeneity in insula and cerebellum: a resting-state fMRI study in patients with major depression and subjects at high risk for major depression. *Psychiatry Research* **182**, 211–215.

Marsman A, Mandl RCW, Klomp DWJ, Bohlken MM, Boer VO, Andreychenko A, Cahn W, Kahn RS, Luijten PR, Hulshoff Pol HE (2014). GABA and glutamate in schizophrenia: a 7 T ^{1}H-MRS study. *NeuroImage. Clinical* **6**, 398–407.

Narr KL, Toga AW, Szeszko P, Thompson PM, Woods RP, Robinson D, Sevy S, Wang Y, Schrock K, Bilder RM (2005). Cortical thinning in cingulate and occipital cortices in first episode schizophrenia. *Biological Psychiatry* **58**, 32–40.

Onitsuka T, McCarley RW, Kuroki N, Dickey CC, Kubicki M, Demeo SS, Frumin M, Kikinis R, Jolesz FA, Shenton ME (2007). Occipital lobe gray matter volume in male patients with chronic schizophrenia: a quantitative MRI study. *Schizophrenia Research* **92**, 197–206.

Palaniyappan L, Al-Radaideh A, Mougin O, Gowland P, Liddle PF (2013*a*). Combined white matter imaging

suggests myelination defects in visual processing regions in schizophrenia. *Neuropsychopharmacology* **38**, 1808–1815.

Palaniyappan L, Liddle PF (2014). Diagnostic discontinuity in psychosis: a combined study of cortical gyrification and functional connectivity. *Schizophrenia Bulletin* **40**, 675–684.

Palaniyappan L, Simmonite M, White TP, Liddle EB, Liddle PF (2013*b*). Neural primacy of the salience processing system in schizophrenia. *Neuron* **79**, 814–828.

Power JD, Barnes KA, Snyder AZ, Schlaggar BL, Petersen SE (2012). Spurious but systematic correlations in functional connectivity MRI networks arise from subject motion. *Neuroimage* **59**, 2142–2154.

Schnack HG, Kahn RS (2016). Detecting neuroimaging biomarkers for psychiatric disorders: sample size matters. *Frontiers in Psychiatry* **7**.

Schobel SA, Chaudhury NH, Khan UA, Paniagua B, Styner MA, Asllani I, Inbar BP, Corcoran CM, Lieberman JA, Moore H, Small SA (2013). Imaging patients with psychosis and a mouse model establishes a spreading pattern of hippocampal dysfunction and implicates glutamate as a driver. *Neuron* **78**, 81–93.

Shen H, Wang L, Liu Y, Hu D (2010). Discriminative analysis of resting-state functional connectivity patterns of schizophrenia using low dimensional embedding of fMRI. *NeuroImage* **49**, 3110–3121.

Taylor SF, Tso IF (2015). GABA abnormalities in schizophrenia: a methodological review of *in vivo* studies. *Schizophrenia Research* **167**, 84–90.

Turner JA, Damaraju E, van Erp TGM, Mathalon DH, Ford JM, Voyvodic J, Mueller BA, Belger A, Bustillo J, McEwen S, Potkin SG, FBIRN, Calhoun VD (2013). A multi-site resting state fMRI study on the amplitude of low frequency fluctuations in schizophrenia. *Frontiers in Neuroscience* **7**.

Venkataraman A, Whitford TJ, Westin C-F, Golland P, Kubicki M (2012). Whole brain resting state functional connectivity abnormalities in schizophrenia. *Schizophrenia Research* **139**, 7–12.

Wang H, Zeng L-L, Chen Y, Yin H, Tan Q, Hu D (2015). Evidence of a dissociation pattern in default mode subnetwork functional connectivity in schizophrenia. *Scientific Reports* **5**.

Woodward ND, Karbasforoushan H, Heckers S (2012). Thalamocortical dysconnectivity in schizophrenia. *American Journal of Psychiatry* **169**, 1092–1099.

Wynn JK, Green MF, Engel S, Korb A, Lee J, Glahn D, Nuechterlein KH, Cohen MS (2008). Increased extent of object-selective cortex in schizophrenia. *Psychiatry Research – Neuroimaging* **164**, 97–105.

Xu Y, Zhuo C, Qin W, Zhu J, Yu C (2015). Altered spontaneous brain activity in schizophrenia: a meta-analysis and a large-sample study. *BioMed Research International* **2015**, e204628.

Yang GJ, Murray JD, Repovs G, Cole MW, Savic A, Glasser MF, Pittenger C, Krystal JH, Wang X-J, Pearlson GD, Glahn DC, Anticevic A (2014). Altered global brain signal in schizophrenia. *Proceedings of the National Academy of Sciences USA* **111**, 7438–7443.

Yu R, Chien Y-L, Wang H-LS, Liu C-M, Liu C-C, Hwang T-J, Hsieh MH, Hwu H-G, Tseng W-YI (2014). Frequency-specific alternations in the amplitude of low-frequency fluctuations in schizophrenia. *Human Brain Mapping* **35**, 627–637.

Yu R, Hsieh MH, Wang H-LS, Liu C-M, Liu C-C, Hwang T-J, Chien Y-L, Hwu H-G, Tseng W-YI (2013). Frequency dependent alterations in regional homogeneity of baseline brain activity in schizophrenia. *PLoS ONE* **8**, e57516.

Zang Y, Jiang T, Lu Y, He Y, Tian L (2004). Regional homogeneity approach to fMRI data analysis. *NeuroImage* **22**, 394–400.

Zhuo C, Zhu J, Qin W, Qu H, Ma X, Tian H, Xu Q, Yu C (2014). Functional connectivity density alterations in schizophrenia. *Frontiers in Behavioral Neuroscience* **8**.

Zou Q-H, Zhu C-Z, Yang Y, Zuo X-N, Long X-Y, Cao Q-J, Wang Y-F, Zang Y-F (2008). An improved approach to detection of amplitude of low-frequency fluctuation (ALFF) for resting-state fMRI: fractional ALFF. *Journal of Neuroscience Methods* **172**, 137–141.

Zuo X-N, Di Martino A, Kelly C, Shehzad ZE, Gee DG, Klein DF, Castellanos FX, Biswal BB, Milham MP (2010). The oscillating brain: complex and reliable. *NeuroImage* **49**, 1432–1445.